Chemical Physics 132 (1989) 219–234
North-Holland, Amsterdam

PROMPT FLUORESCENCE FROM BIPHENYLENE IN LIQUID SOLUTION: ABSENCE OF DETECTABLE $S_2 \rightarrow S_0$ FLUORESCENCE AND ITS IMPLICATIONS, VIBRATIONAL STRUCTURE AND POLARIZATION OF $S_1 \rightarrow S_0$ FLUORESCENCE, AND ORIENTATIONAL RELAXATION OF MOLECULES IN S_1

Bernhard NICKEL and Joachim HERTZBERG
Max-Planck-Institut für Biophysikalische Chemie, Abteilung Spektroskopie, Am Fassberg, D-3400 Göttingen, FRG

Received 7 September 1988

The prompt emission from $S_0 \rightarrow S_2$ photoexcited biphenylene in 3-methylpentane has been investigated. No prompt $S_2 \rightarrow S_0$ fluorescence has been observed. The implications of this negative result are discussed. It is shown that lengthening of the radiative lifetime of S_2 due to intermediate strong S_2–S_1 coupling is the likely cause of the absence of detectable $S_2 \rightarrow S_0$ fluorescence. The observable resonance Raman lines of biphenylene can be assigned to totally symmetric vibrations. The position of $S_{1,0}$ is determined by a vibrational analysis of the $S_1 \rightarrow S_0$ fluorescence. The polarization degree P of the $S_1 \rightarrow S_0$ fluorescence is positive. From the dependence of P on temperature and viscosity, orientational relaxation times of biphenylene in S_1 are determined with Perrin's formula.

1. Introduction

The antiaromatic hydrocarbon biphenylene has unusual photophysical properties [1]. In this paper we investigate several aspects of the *prompt* fluorescence and the resonance Raman scattering of biphenylene in liquid solution; the *delayed* luminescence of biphenylene in liquid solution is treated in the following paper [2].

The starting point of our investigation was the original version of a paper by Elsaesser et al. [1] on the transient absorption of biphenylene in liquid solution. Upon photoexcitation of biphenylene to the second excited singlet state (S_2) these authors observed a biexponentially decaying transient absorption with the time constants $\tau' = 8 \pm 3$ ps and $\tau'' = 250 \pm 40$ ps. There has been no doubt in the assignment of the slow component to $S_1 \rightarrow S_i$ absorption ($\tau'' = \tau_1$). The interpretation of the fast component has been less obvious. After discussion of various conceivable interpretations, Elsaesser et al. came to the conclusion that the fast component had to be assigned to transient $S_2 \rightarrow S_j$ absorption ($\tau' = \tau_2$). For the correctness of this assignment, the observability of an $S_2 \rightarrow S_0$ fluorescence seemed to be a necessary condition, for the following reason. For the lifetime τ_1 of the first excited singlet state of many aromatic compounds the relation $\tau_1 \approx \tau^*_{1r} \phi_{1f}$ holds [3], where τ^*_{1r} is the radiative lifetime of S_1 calculated from the $S_0 \rightarrow S_1$ absorption band and ϕ_{1f} is the quantum yield of the $S_1 \rightarrow S_0$ fluorescence. If one assumes [4–13] that the analogous relation

$$\tau_n \approx \tau^*_{nr} \phi_{nf} \tag{1}$$

holds for the lifetime τ_n of upper excited singlet states S_n ($n \geqslant 2$), then in the present case from $\tau_2 \approx 8$ ps and $\tau^*_{2r} \approx 16$ ns (cf. section 3.2) one would obtain $\phi_{2f} \approx 5 \times 10^{-4}$. Thus one would expect an $S_2 \rightarrow S_0$ fluorescence with an intensity similar to that of the $S_1 \rightarrow S_0$ fluorescence ($\phi_{1f} \approx 2.3 \times 10^{-4}$ [1]). For experimental reasons in the investigation [1] no reliable information on the $S_2 \rightarrow S_0$ fluorescence was obtained. When the fluorescence quantum yield is very small, the main experimental problem is the measurement of the emission spectrum of a sample with a spectral resolution high enough for the distinction between Raman bands and fluorescence bands. Incidentally, our equipment has been suitable for this purpose, and the first aim of this investigation has been to obtain a reliable estimate of ϕ_{2f}.

The absence of a detectable $S_2 \rightarrow S_0$ fluorescence ($\phi_{2f} \lesssim 1 \times 10^{-6}$) seemed to be in contradiction with the assignment of the fast component of the transient absorption of biphenylene in ref. [1]. However, it has turned out that, with respect to the implications of the low value of ϕ_{2f}, the fault need not be with the assignment of the fast component of the transient absorption. Since the energy gap between S_1 and S_2 is not large (≈ 4000 cm^{-1}), intermediate strong S_2–S_1 coupling is expected to be important, and the true radiative lifetime τ_{2r} of S_2 can be much longer than the value of τ_{2r}^* obtained from the $S_0 \rightarrow S_2$ absorption band. This point has been briefly treated in ref. [1]. In this paper we discuss in more detail the consequences of intermediate strong S_1–S_2 coupling and of the inapplicability of eq. (1).

In the second main part of this paper we treat several aspects of the $S_1 \rightarrow S_0$ fluorescence from biphenylene. The first point of interest has been the position of $S_{1,0}$. Biphenylene belongs to the point group D_{2h}, and S_1 belongs to the irreducible representation B_{3g}[#1]. The purely electronic one-photon transition $S_{0,0}(A_g) \leftrightarrow S_{1,0}(B_{3g})$ is symmetry forbidden [15] and neither in absorption nor in emission observable. We shall determine the position of $S_{1,0}$ by a vibrational analysis of the spectrum of the $S_1 \rightarrow S_0$ fluorescence. The second point of interest has been the polarization of this fluorescence. The observable part of the $S_0 \rightarrow S_1$ absorption band [15–18] has the same long-axis polarization as the $S_0 \rightarrow S_2$ absorption band – as expected for S_1–S_2 vibronic coupling [19]. If the S_1–S_2 vibronic coupling is dominant also in the observable $S_1 \rightarrow S_0$ fluorescence (as concluded from the vibrational analysis), then upon excitation of biphenylene to S_2 this fluorescence should be long-axis polarized, and a positive polarization degree P should be observed. Thus our second aim was to measure the polarization spectrum $P(\tilde{\nu})$ of the $S_1 \rightarrow S_0$ fluorescence from biphenylene. The third point of interest has been the orientational relaxation time τ_{or} of biphenylene in S_1 which can be obtained with Perrin's formula [20] from the dependence of P on solvent viscosity and temperature, if the lifetime τ_1 of S_1 is known. A knowledge of τ_{or} has been useful in connection with the following problems. Firstly, according to the theoretical calculations of ref. [1], a predominant *long-axis* polarization of the observable transient $S_2 \rightarrow S_j$ and $S_1 \rightarrow S_i$ absorption is expected. Hence, transient-absorption experiments designed for the determination of P and τ_{or} should yield also a positive value of P and roughly the same value of τ_{or} as that obtained from fluorescence depolarization. Secondly, in connection with the problem of detecting a prompt $S_2 \rightarrow S_0$ fluorescence, the relaxation time of a specific environment of a solute molecule is of interest; τ_{or} is a rough measure for this relaxation time. Finally, in connection with the delayed excimer fluorescence from biphenylene [2], the ratio τ_{or}/τ_1 has been important.

2. Experimental

Substances. Biphenylene was of the same quality as in ref. [1]. 3-methylpentane (Fluka 68322, 99%) was rectified over a 1 m column and chromatographed with basic aluminium oxide immediately before use.

Samples. For the measurement of the low-temperature absorption spectrum of biphenylene, units of four connected cylindrical absorption cuvettes with different optical path lengths were used [21]. For the measurement of the fluorescence spectrum a special fluorescence flow cell with a solution volume of ≈ 0.2 dm^3 was used [22]; the cross section of the actual flow cell was 3 mm × 10 mm. Samples were prepared as described in ref. [23].

Absorption spectrum. For the measurement of the low-temperature absorption spectrum of biphenylene a home-made optical cryostat and a home-made absorption spectrometer [21] were used.

Emission spectrum. A spectrometer for the measurement of prompt or delayed luminescences was used. The sample was excited with the linearly polarized light of the UV lines at 351.1 and 351.4 nm of an argon ion laser (Spectra Physics 2025). The fluorescence was observed in a direction perpendicular to the electric vector of the excitation light (see fig. 1). The polarization-dependent sensitivity of the spectrofluorimeter was eliminated with a Hanle depolarizer (B. Halle, Berlin, PHD 25). In the spectral range of the Raman bands, the emission spectrum was

---

[#1] In part of the literature the symmetry notation B_{1g} has been used for S_1. The present notation B_{3g} is in accord with Mulliken's recommendation REC 5b [14]: The x axis is perpendicular to the plane of the molecule, and the z axis cuts the greatest number of bonds.

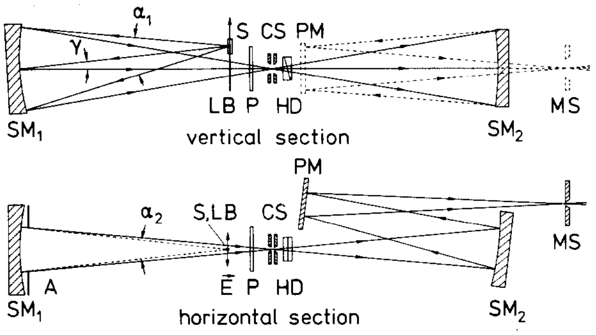

Fig. 1. Experimental arrangement for the measurement of the polarization of the $S_1 \rightarrow S_0$ fluorescence. A: rectangular aperture (the aperture angle α_2 is drawn enlarged by a factor of 2.5); CS: chopper slits; $\vec{E}$: polarization of excitation light; HD: Hanle depolarizer; LB: laser beam; MS: monochromator slit; P: dichroic sheet polarizer; PM: plane mirror; S: sample; SM: spherical mirror. The cross section of the sample (fluorescence flow cell) is 3 mm × 10 mm. For the measurement of emission spectra the aperture A and the polarizer P are removed. The chopper was used for the measurement of delayed luminescences; for details cf. ref. [2].

measured with a spectral resolution of ≈ 0.2 nm; at longer wavelengths the spectral resolution was ≈ 0.4 nm. The emission spectrum was corrected as described in ref. [24].

Fluorescence polarization. For the measurement of fluorescence polarization, a dichroic sheet polarizer was inserted as polarization analyzer in the emission light beam (Spindler & Hoyer, type 10 K, relative transmission of pair of crossed polarizers $< 10^{-3}$). The measured quantity was the dichroic ratio

$$d = I_{\parallel}/I_{\perp} , \tag{2}$$

where $I_{\parallel}$ and $I_{\perp}$ denote the intensities of the fluorescence for parallel and perpendicular orientation of the analyzer relative to the polarization of the excitation light. The polarization degree P is defined by

$$P = (d-1)/(d+1) . \tag{3}$$

For the given polarizaton of the excitation light, d does not sensitively depend on the off-axis angle γ or on the aperture angle α_1, as long as the emission is observed in a direction perpendicular to the polarization of the excitation light (see fig. 1). On the other hand, a finite aperture angle α_2 leads to an error in d, since it is equivalent to a spread of the polarization direction of the excitation light; by this error $|P|$ is decreased. Therefore α_2 was limited by a rectangular aperture to $\approx 5°$. The finite off-axis angle ($\gamma \approx 7°$) led to $d_u = 0.9915 \neq 1$ for unpolarized light, and in principle P had to be calculated with the corrected value $d = d'/d_u$, where d' was the measured value. For practical reasons we calculated corrected values of P with the equation $P = P' - P_u$ with $P_u = -0.0043$; because of the smallness of $1 - d_u$, the maximal relative error of P resulting from this inaccurate correction was -0.3%.

Viscosity. The viscosity of 3-methylpentane was measured with an improved capillary viscosimeter similar to that described in ref. [25]. The uniformity of the capillary temperature was better than ± 0.1 K, and the absolute temperature (T_{68} temperature scale [26]) was known with an accuracy better than ± 0.1 K. In the temperature range from 115 to 293 K, the temperature dependence of the viscosity η can be represented by the following empirical formula within the absolute accuracy $\pm 0.5\%$ of the experimental data:

$$\log_{10}(\eta/\mathrm{cP}) = \sum_{n=0}^{3} B_n (T-C)^{-n} , \tag{4}$$

where $B_0 = -1.77749$, $B_1 = 3.86069 \times 10^2$ K, $B_2 = -2.43540 \times 10^4$ K^2, $B_3 = 1.13891 \times 10^6$ K^3 and $C = 50.90$ K.

Density. The density ρ of 3-methylpentane was measured with an absolute accuracy better than $\pm 0.1\%$. Between 98 and 293 K, the experimental values of ρ can be represented with an accuracy of $\pm 0.03\%$ by the formula

$$\rho = A_0 + A_1 T + A_2 T^2 + A_3 T^3 , \tag{5}$$

where $A_0 = 0.92735$ g cm^{-3}, $A_1 = -1.0730 \times 10^{-3}$ g cm^{-3} K^{-1}, $A_2 = 1.2415 \times 10^{-6}$ g cm^{-3} K^{-2}, $A_3 = -2.1896 \times 10^{-9}$ g cm^{-3} K^{-3}.

Refractive index. The dependence of the refractive index n of 3-methylpentane on wavelength and temperature was estimated with eq. (8) of ref. [24]. Apart from ρ of 3-methylpentane, the same parameter values as for isopentane were used.

3. On the $S_2 \rightarrow S_0$ fluorescence

3.1. Upper limit of the quantum yield of the prompt $S_2 \rightarrow S_0$ fluorescence

We measured the emission spectrum of a 1.0×10^{-4} M solution of biphenylene in 3-methylpentane at 130

K. Biphenylene was excited to S_2 at $\approx 28500\ \mathrm{cm}^{-1}$ – close to the excitation wavenumber $28200\ \mathrm{cm}^{-1}$ used in the transient-absorption experiments of ref. [1] (see absorption spectrum in fig. 2). Three components of the emission spectrum (fig. 3) are easy to discern: the Rayleigh line at $\approx 28500\ \mathrm{cm}^{-1}$, Raman bands between 25000 and $28300\ \mathrm{cm}^{-1}$, and the $S_1 \rightarrow S_0$ fluorescence band between 14500 and $23500\ \mathrm{cm}^{-1}$.

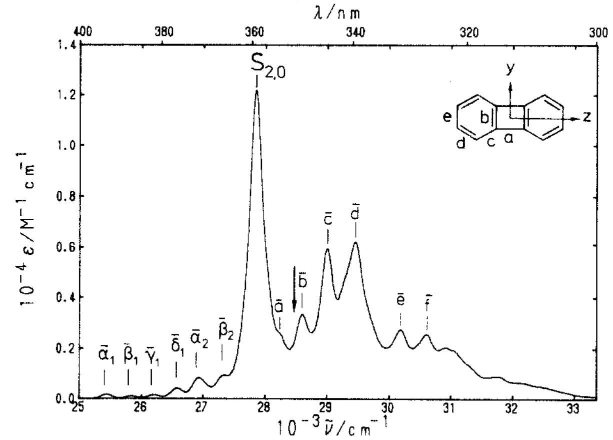

Fig. 2. Absorption spectrum of biphenylene in 3-methylpentane at 100 K. The arrow denotes the excitation wavenumber; for the assignment of the vibronic contour bands ā, b̄, ..., cf. table 2, and of $\bar{\alpha}_1, \bar{\beta}_1, \ldots$, cf. section 4.1.

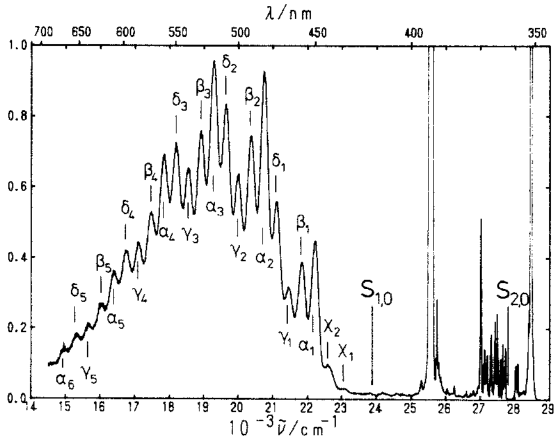

Fig. 3. Corrected emission spectrum of a solution of biphenylene (1.0×10^{-4} M) in 3-methylpentane at 130 K. The solution was excited with the UV lines of an argon ion laser at 351.1 and 351.4 nm (intensity ratio $\approx 2{:}1$). The vertical bars only approximately denote the positions of the vibronic bands of the $S_1 \rightarrow S_0$ fluorescence.

An enlarged view of the Raman bands is shown in fig. 4. By comparing this spectrum with the Raman spectrum of pure 3-methylpentane, some of the lines can be unambiguously assigned to the resonance Raman spectrum of biphenylene (see arrows in fig. 4). For an accurate determination of the corresponding vibrational wavenumbers the spectrum in fig. 4 is not suitable, since the spectral resolution was not high enough for the resolution of the Raman doublets resulting from the excitation with *two* UV lines of the argon ion laser (351.1 and 351.4 nm, intensity ratio $\approx 2{:}1$). Nevertheless one can show that – within the limited accuracy of our data – the observed resonance Raman lines are in agreement with the known ground-state vibrations of biphenylene [27]. At the given spectral resolution and the given intensity ratio of the excitation lines, the effective average excitation wavenumber was $\tilde{\nu}_{\mathrm{exc}} = 28476\ \mathrm{cm}^{-1}$ (we neglect small effects resulting from the use of wavelengths measured in air). The corresponding resonance-Raman vibrational wavenumbers are listed in table 1. All eight identified resonance Raman lines of biphenylene can be assigned to totally symmetric vibrations. Of the ten totally symmetric fundamentals[#2] only three are observed; the remaining seven

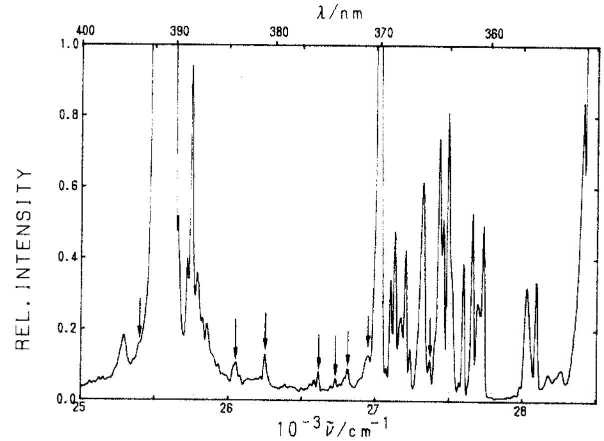

Fig. 4. Enlarged representation of the Raman region of the emission spectrum of fig. 3. The arrows denote the resonance Raman lines of biphenylene which are assigned in table 1.

[#2] Throughout this paper, vibrational fundamentals from ref. [27] are denoted by ν, and measured wavenumbers are denoted by $\tilde{\nu}$.

Table 1
Assignment of resonance Raman lines of biphenylene in 3-methylpentane at 130 K. ν_n: wavenumbers of the totally symmetric ground-state fundamentals [27]; $\tilde{\nu}_{RR}$: vibrational wavenumbers of the resonance Raman lines referring to an effective excitation wavenumber $\tilde{\nu}_{exc}=28476$ cm^{-1}; $\Delta\tilde{\nu}$: deviation of $\tilde{\nu}_{RR}$ from assignment

n	ν_n (cm^{-1})	$\tilde{\nu}_{RR}$ (cm^{-1})	$\Delta\tilde{\nu}$ (cm^{-1})
1	3074	3080	+6
2	3057		
3+9		2427	−4
4+9		2227	0
7+9		1865	−5
8+9		1748	−6
3	1666	1664	−2
9+9		1529	−1
4	1462		
5	1399		
6	1166		
7	1105	1109	+4
8	989		
9	765		
10	395		

fundamentals coincide with strong Raman lines of the solvent. The five other observed lines are combinations of two totally symmetric fundamentals, one of them always being $\nu_9(a_g)$ (765 cm^{-1} [27]). Another aspect of the resonance Raman spectrum of biphenylene is discussed in section 3.3.

No indication of an $S_2\rightarrow S_0$ fluorescence band has been found. Reabsorption cannot be responsible for the nonobservability of this fluorescence, though the minimum in the emission spectrum at ≈27800 cm^{-1} roughly coincides with the maximum of the $S_0\rightarrow S_2$ absorption band at 27850 cm^{-1} (cf. fig. 2). The average path length of the emitted light in the sample was ≈0.15 cm, which corresponded at the given concentration of biphenylene to a maximal attenuation of the emitted light by a factor of ≈0.6 at 27850 cm^{-1}.

In the following we try to obtain an *upper limit* of the relative quantum yield of the S_2 fluorescence. For the present, we assume that the $S_2\rightarrow S_0$ fluorescence band is symmetric to the $S_0\rightarrow S_2$ absorption band and that the maxima of both bands nearly coincide. This assumption is in part justified by the observed spectrum of the delayed $S_2\rightarrow S_0$ fluorescence [2]; for a more detailed discussion of the likely spectrum of the prompt $S_2\rightarrow S_0$ fluorescence cf. section 3.3. The resulting hypothetical spectrum of the prompt $S_2\rightarrow S_0$ fluorescence as depicted in fig. 5 corresponds to the maximal $S_2\rightarrow S_0$ fluorescence intensity compatible with the observed emission spectrum. The integrated intensities of the hypothetical $S_2\rightarrow S_0$ fluorescence band and of the measured $S_1\rightarrow S_0$ fluorescence band in fig. 5 correspond to the quantum-yield ratio

$$r=\phi_{2f}/\phi_{1f}\approx 4\times 10^{-3}\,. \tag{6}$$

In connection with ref. [1], the value of r at 293 K is needed. We assume that ϕ_{2f} is practically independent of the temperature. An estimate of the ratio

$$g=\phi_{1f}(293\ \mathrm{K})/\phi_{1f}(130\ \mathrm{K}) \tag{7}$$

can be obtained from a comparison of the emission spectra at 293 K (fig. 6) and 130 K (fig. 5). By using the integrated intensity of the group of C–H Raman bands at 25550 cm^{-1} as internal intensity standard, one can see that $0.7<g<1.0$. Thus, for the purpose of this rough estimate, ϕ_{1f} and r can be assumed to be independent of temperature (a detailed estimate of the temperature dependence of the lifetime τ_1 of S_1 is made in section 4.2). Finally, with $\phi_{1f}=2.3\times 10^{-4}$

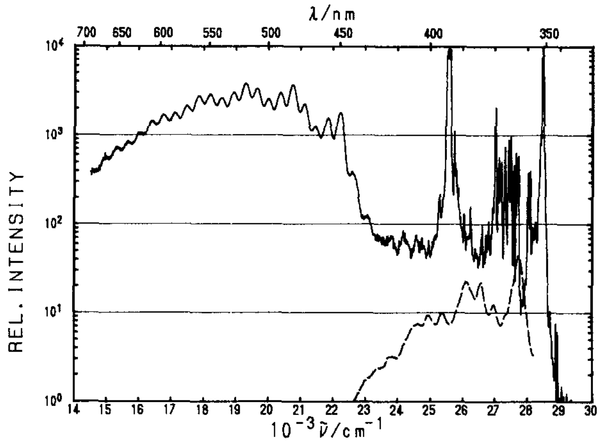

Fig. 5. Logarithmic plot of the emission spectrum of fig. 3. The dashed spectrum is the mirror image of the $S_0\rightarrow S_2$ absorption band (mirror wavenumber: 27800 cm^{-1}). The relative integrated intensities of the two spectra correspond to the quantum yield ratio $\phi_{2f}/\phi_{1f}\approx 4\times 10^{-3}$.

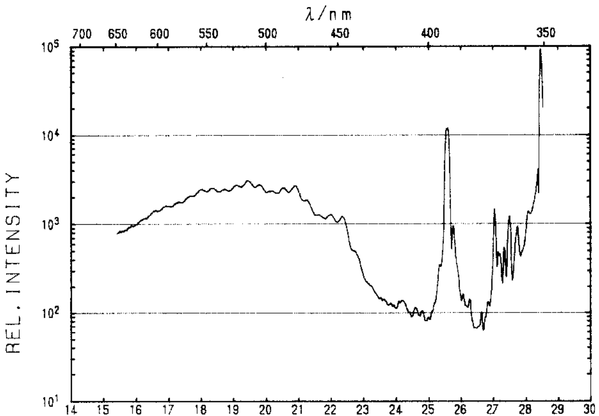

Fig. 6. Corrected emission spectrum of a solution of biphenylene (1.0×10^{-4} M) in 3-methylpentane at 293 K (same sample and same excitation as in fig. 3). The Raman region of the spectrum was measured with lower resolution than that of the spectrum of fig. 5.

[1], we obtain[#3]

$$\phi_{2f} \lesssim 1\times10^{-6}\,. \tag{8}$$

The negative result of our attempt to detect the *prompt* $S_2 \rightarrow S_0$ fluorescence from biphenylene illustrates the statement in ref. [22] that in general with one-photon $S_0 \rightarrow S_n$ excitation ($n > 1$) it is not possible to detect the prompt $S_n \rightarrow S_0$ fluorescence. However, this fluorescence may be detectable as *delayed fluorescence*, if the energy of two metastable triplet states is sufficient for the population of S_n by triplet-triplet annihilation [9]. We have been able to measure apart from the delayed $S_1 \rightarrow S_0$ fluorescence also a very weak delayed fluorescence with $S_2 \rightarrow S_0$ character [2]; the ratio of the integrated intensities of both delayed fluorescences is $r_{df} \approx 10^{-3}$. This value can be considered as reliable *lower limit* of r (cf. ref. [2]). Thus our final estimate of ϕ_{2f} is

$$2\times10^{-7} \lesssim \phi_{2f} \lesssim 1\times10^{-6}\,. \tag{9}$$

3.2. Implications of the low quantum yield of the $S_2 \rightarrow S_0$ fluorescence

The original idea of this investigation was to use eq. (1) for an estimate of the lifetime τ_2 of S_2. Since the spectrum of the S_2 fluorescence was not known, we used for the calculation of τ^*_{2r} Förster's equation (eq. (32,6′) in ref. [28], identical with eq. (4.21) in ref. [29]), in which mirror symmetry between absorption band and fluorescence band is explicitly assumed. With the absorption spectrum of fig. 2, with a mirror wavenumber $\tilde{\nu}_0 = 27800$ cm^{-1}, with an estimated refractive index $n \approx 1.54$ of 3-methylpentane at 100 K, and with integration from 27400 to 33500 cm^{-1}, we obtained $\tau^*_{2r} \approx 16$ ns. From this value and from the upper limit of ϕ_{2f} an upper limit of ≈ 16 fs would result for the lifetime of S_2. The purpose of this section is to show that the lifetime of S_2 cannot be determined in this way.

The main criteria for the applicability of eq. (1) are the size of a molecule and the magnitude of the energy gap $\Delta E_{n,n-1}$ between S_n and S_{n-1}. Eq. (1) can be valid only if a separate $S_0 \rightarrow S_n$ transition is observable. In practice this means, the $S_0 \rightarrow S_n$ absorption band must not appreciably overlap with the $S_0 \rightarrow S_{n-1}$ absorption band. With large molecules of the size of biphenylene, typically this is the case for $\Delta E_{n,n-1} \gtrsim 6000$ cm^{-1} [30]. In the theory of radiationless transitions, this corresponds to the *statistical limit* of S_n–S_{n-1} coupling [30–33]. For aromatic hydrocarbons this criterion is fulfilled always for $n = 1$, in rare cases for $n = 2$, and probably never for $n \geqslant 3$.

If $\Delta E_{n,n-1}$ is considerably smaller than 6000 cm^{-1}, then intramolecular coupling of S_n with S_{n-1} may lead to new mixed molecular eigenstates. We restrict the following consideration to the case of a weak (forbidden) $S_0 \rightarrow S_1$ transition and an allowed $S_0 \rightarrow S_2$ transition [34], and here to the special case of *intermediate strong coupling* [31–35]. In this case, the pure zero-order vibrationless state $S_{2,0}$ mixes with $N-1$ zero-order vibronic states $S_{1,u}$ of the same symmetry; the resulting mixed vibronic states $S^{2,0}_{1,i}$ ($i = 1, 2, ..., N$) of S_1 and S_2 parentage are observed. Thus the zero-order 0, 0 transition $S_{0,0} \rightarrow S_{2,0}$ is replaced by a multiplet of N vibronic transition $S_{0,0} \rightarrow S^{2,0}_{1,i}$, each carrying on the average only $1/N$ of the oscillator strength of the pure zero-order transition. In a similar way, zero-order vibronic transitions $S_{0,0} \rightarrow S_{2,v}$ are replaced by

---

[#3] In ref. [1] the value 3×10^{-6} is used as upper limit of ϕ_{2f}. We originally proposed this value in order to allow for the possibility that the spectrum of the $S_2 \rightarrow S_0$ fluorescence might strongly deviate from the expected mirror-symmetric form. However, this precaution is no longer necessary, since the assumption of a mirror-symmetric intensity distribution has been justified by the observed delayed $S_2 \rightarrow S_0$ fluorescence [2].

multiplets of mixed vibronic transitions $S_{0,0} \rightarrow S_{1,i+v}^{2,v}$. The relation between the average radiative lifetime τ_{2r} of the states $S_{1,i}^{2,0}$ and the radiative lifetime τ_{2r}^{*} calculated from the total $S_0 \rightarrow S_2$ absorption band is then given by

$$\tau_{2r} \approx N \tau_{2r}^{*} . \tag{10}$$

With this definition of N, two relations are obtained:

$$\tau_2^{-1} \approx (N \tau_{2r}^{*})^{-1} + k_{2n} , \tag{11}$$

where k_{2n} is the rate constant for the nonradiative decay[#4] of $S_{1,i}^{2,0}$ to S_1, and

$$N \approx \tau_2 (\tau_{2r}^{*} \phi_{2f})^{-1} . \tag{12}$$

S_2–S_1 level mixing has been known since long for naphthalene and other aromatic compounds. However, since the basic facts do not seem to be widely known, we list some key references for naphthalene and phenanthrene.

(a) McClure [36] investigated the absorption spectrum of naphthalene in a durene host crystal. In the spectral range of the expected $S_0 \rightarrow S_2$ absorption band, he found many sharp lines resulting from S_2–S_1 level mixing. Wessel and McClure [37] were able to give a qualitatively satisfactory quantum mechanical explanation of the observed mixed vibronic multiplets. Many of the observed sharp lines had widths (fwhm) of less than 2 cm^{-1}, corresponding to lifetimes of more than 2 ps. Another important aspect of the work of Wessel and McClure is mentioned in section 3.3. Robinson and Langhoff [38,39] succeeded in a nearly quantitative theoretical description of the observed spectra. Fischer [40] reviewed this work.

(b) A lengthening of the radiative lifetime of S_2 due to the S_2–S_1 level mixing has been explicitly postulated [34,41,42]. Eq. (11) shows that in principle even the extreme case $\tau_2 > \tau_{2r}^{*}$ is possible, if k_{2n} is unusually small. For small molecules this case is experimentally well established [43]. For aromatic compounds, however, there is no really convincing example of this extreme case. The reported long-lived strong $S_2 \rightarrow S_0$ fluorescence from naphthalene vapour [42] is in contradiction with the negative results obtained by other research groups [5,44–46].

(c) Beck et al. [47] investigated the absorption of jet-cooled naphthalene and observed a repeated multiplet of vibronic $S_{0,0} \rightarrow S_{1,i+v}^{2,v}$ transitions. From linewidth measurements they obtained rate constants for the intramolecular vibrational relaxation (IVR) as a function of the excess energy E_{exc} relative to $S_{1,0}$. The values range from $k_{\text{IVR}} = 9 \times 10^{10}$ s^{-1} for $E_{\text{exc}} = 3068$ cm^{-1} (still in the range of the $S_0 \rightarrow S_1$ absorption band) to $k_{\text{IVR}} = 7 \times 10^{11}$ s^{-1} for $E_{\text{exc}} = 5200$ cm^{-1} (in the range of the $S_0 \rightarrow S_2$ absorption band). These results support the idea [34,42] that, in *isolated* molecules, there is no fundamental difference in the IVR rates of pure S_1 vibronic states and mixed S_2–S_1 vibronic states of the same energy. The absolute values of k_{IVR} are, however, more than 1000 times greater than those reported in ref. [42].

(d) The transition from strong intermediate coupling to the statistical limit may critically depend on the energy difference $\Delta E_{2,1}$ between S_2 and S_1. Fischer [40,48] observed S_2–S_1 level mixing of phenanthrene in a durene host crystal ($\Delta E_{2,1} \approx 4700$ cm^{-1}). Amirav et al. [30] found no S_2–S_1 level mixing with jet-cooled phenanthrene ($\Delta E_{2,1} = 6051$ cm^{-1}); that means, for the isolated phenanthrene molecule the statistical limit [30–33] is reached.

Intermediate strong S_2–S_1 coupling is a general phenomenon in the sense that it critically depends only on the density of S_1 vibronic states at the energy of $S_{2,0}$. Thus, in this respect there should be no fundamental difference between the *antiaromatic* hydrocarbon biphenylene and the *aromatic* hydrocarbon naphthalene and phenanthrene. With respect to the number of atoms and the value of $\Delta E_{2,1}$, biphenylene (20 atoms, $\Delta E_{2,1} \approx 4000$ cm^{-1} in alkanes – cf. section 4.1) lies between naphthalene (18 atoms, $\Delta E_{2,1} \approx 3300$ cm^{-1} in alkanes) and phenanthrene (24 atoms, $\Delta E_{2,1} \approx 5000$ cm^{-1} in alkanes). Hence in biphenylene intermediate strong S_2–S_1 coupling can be expected. Detailed high-resolution investigations of the S_2 absorption band of biphenylene are not known to us, but there are two indications in the literature on S_2–S_1 level mixing. Hochstrasser and McAlpine [49] mention the observation of a few sharp lines in the range of the S_2 absorption band of biphenylene in a biphenyl host crystal. Zanon [17] observed sharp lines with an estimated half-width of 2–3 cm^{-1} in the range of the S_2 absorption band of biphenylene va-

---

[#4] Note that dephasing of the initially prepared states is not considered as a decay process as long as the S_2 character of the mixed vibronic states is preserved.

pour. In conclusion, there is no doubt that biphenylene in S_2 should exhibit a behaviour similar to that of naphthalene. Thus, the assignment of the fast component of the transient absorption of biphenylene to $S_2 \rightarrow S_j$ absorption ($\tau' \equiv \tau_2$) [1] need not be in contradiction to the low quantum yield of the $S_2 \rightarrow S_0$ fluorescence. With $\tau_2 \approx 8$ ps, $\tau^*_{2r} \approx 16$ ns, and the upper and lower limits (9) of ϕ_{2f}, eq. (12) yields $500 \lesssim N \lesssim 2500$. Too great values of N are obtained, if ϕ_{2f} is too small and/or τ_2 is too long. In the following we consider both possibilities.

The absence of a detectable prompt $S_2 \rightarrow S_0$ fluorescence from biphenylene may seem surprising, since some of the diphenylpolyenes with an analogous ordering of excited states, $S_1(A_g)$ and $S_2(B_u)$, exhibit a prompt $S_2 \rightarrow S_0$ fluorescence [50–52]. However, a closer inspection reveals substantial differences between biphenylene and the diphenylpolyenes. We confine the discussion to 1,6-diphenylhexa-1,3,5-triene (DPH). Isolated DPH molecules in the gas phase ($\Delta E_{2,1} \approx 3400$ cm^{-1} [53]) obviously represent the case of intermediate *strong* coupling; hence the absence of a detectable $S_2 \rightarrow S_0$ fluorescence [53] is not surprising. DPH in hexane ($\Delta E_{2,1} \approx 600$ cm^{-1} [52]) represents the case of intermediate *weak* coupling [34]. Thus the observation of a short-lived prompt $S_2 \rightarrow S_0$ fluorescence from DPH in hexane [50] is not surprising. The steady-state $S_2 \rightarrow S_0$ fluorescence is mainly due to the thermally activated repopulation of S_2 [51,52]. Note that the observability of a thermally activated steady-state $S_2 \rightarrow S_0$ fluorescence does not depend on the type of intermediate coupling, since in the case of intermediate strong coupling the increase of the radiative lifetime of S_2 by a factor N is compensated by the simultaneous N-fold degeneracy of S_2.

In the literature there are estimates of *ultrashort* electronic relaxation times τ_n ($10 \lesssim \tau_n \lesssim 100$ fs). In view of these estimates, a lifetime of ≈ 8 ps for S_2 seems to be extremely long. In the following we show that all *indirect* estimates of τ_n are doubtful in the case of obvious S_n–S_{n-1} level mixing. Estimates of τ_n based on fluorescence quantum yields [4–6,8–12] may be wrong because of the inapplicability of eq. (1). Estimates of τ_n based on the comparison of the widths of *inhomogeneously broadened* $S_{0,0} \rightarrow S_{n,0}$ and $S_{0,0} \rightarrow S_{1,0}$ absorption bands [7–9,12] are in general wrong, since – in contrast to the assumptions made – not the homogeneous width Γ_{hom} of the $S_{0,0} \rightarrow S_{n,0}$ transition is obtained but the spread of the $S_{0,0} \rightarrow S^{n,0}_{n-1,i}$ multiplet (for a more detailed discussion of this point cf. section 3.3). Moreover, both methods may yield contradictory results; thus, in the case of biphenylene one obtains $\Gamma_{\text{hom}} \lesssim 240$ cm^{-1} corresponding to $\tau_2 \gtrsim 22$ fs – in contradiction to the estimate $\tau_2 \lesssim 16$ fs based on eq. (1). Hole-burning spectroscopy [13] will also give too small value of τ_n, if the statistical limit is not reached. For a critical discussion of ultrafast electronic relaxation cf. also ref. [54]. A positive aspect of the unreliability of indirectly determined lifetimes of upper excited singlet states is that possibly the upper excited states of many compounds are amenable to available methods of ultrafast spectroscopy [55]. Similar considerations apply to the lifetime of upper triplet states.

Finally, we have to ask whether the term "second excited singlet state" and the symbol S_2 are still appropriate in the case of S_1–S_2 vibronic level mixing. We believe that in *low-resolution* spectroscopy the use of S_2 remains a convenient abbreviation for the S_1–S_2 vibronic multiplets, and we will use the symbol S_2 with this meaning.

3.3. Distinction between $S_2 \rightarrow S_0$ fluorescence and resonance Raman scattering

In this section we try to answer the question whether, in the emission spectrum of biphenylene in 3-methylpentane, $S_2 \rightarrow S_0$ resonance fluorescence (RF) lines can be distinguished from resonance Raman (RR) lines. Let us first compare S_2–S_1 level mixing in isolated molecules, in guest molecules in host crystals, and in solute molecules in a glass. In an isolated molecule the mixed vibronic states $S^{2,v}_{1,i+v}$ are characteristic for the molecule itself. In a guest molecule the observed states $S^{2,v}_{1,i+v}$ depend on both, the nearly host-independent spacing of the vibronic states $S_{1,u}$ and the host-dependent energy difference $\Delta E_{2,1}$ between $S_{2,0}$ and $S_{1,0}$; thus, in different host crystals completely different $S^{2,v}_{1,i+v}$ multiplets are observed [37]. Finally, in a glass there is a whole distribution of solute environments or *sites* (σ) which can be partly characterized by their site-specific energy difference $\Delta E_{2,1}(\sigma)$. Therefore, an observable $S_{0,0} \rightarrow S_{2,v}$ vibronic contour band results from a whole distribution of $S^{2,v}_{1,i+v}$ multiplets.

We now consider the behaviour of biphenylene in 3-methylpentane at two temperatures: (a) $T \leqslant 4$ K: glass; (b) $T = 130$ K: viscous solution, $\eta = 33$ cP. For both temperatures we assume an average lifetime $\tau_2 \approx 8$ ps [1] of the $S^{2,v}_{1,i+v}$ states.

In a low-temperature glass, the zero-phonon RF lines should be narrow lines similar to those known for the narrow-band excited $S_1 \rightarrow S_0$ fluorescence of many compounds [56]. Since the zero-phonon RF lines coincide with the RR lines, a distinction between the two types of lines should be practically impossible.

For the discussion of case (b), a knowledge of the relaxation time τ_σ of a specific solute environment σ is essential. One may assume that τ_σ is of the same order of magnitude as the orientational relaxation time τ_{or} of biphenylene in S_1 (cf. section 4.2). In liquid 3-methylpentane at 130 K, $\tau_{\mathrm{or}} = 1.0 \pm 0.2$ ns is much longer than τ_2. That means, during the lifetime of a state $S^{2,v}_{1,i+v}$, the environment of a biphenylene molecule practically does not change. In this sense, the situation is similar to that of a guest molecule in a glass or a host crystal at the same temperature. At 130 K, the zero-phonon RF line should be very weak, and the phonon sidebands of this line should coalesce to a single band, that is broader than the RR line, but still considerably narrower than a vibronic contour band of the $S_1 \rightarrow S_0$ fluorescence. That means, part of the background of the RR lines has to be assigned to the resonance fluorescence.

Apart from the width of the RF lines, an estimate of their relative intensities is of interest. We confine the following consideration to the strongest RF line. For this purpose a rough vibrational analysis of the $S_0 \rightarrow S_2$ absorption band is necessary. If we assume that only totally symmetric vibrations are important and that the vibrational wavenumbers in S_2 do not much differ from ground-state vibrational wavenumbers, then we can easily assign some of the vibrational contour bands (cf. table 2). On the basis of this analysis one can see that excitation at 28476 cm^{-1} corresponds to predominant population of vibronic states $S^{2,v}_{1,i+v}$ with S_{2,ν_9} character. Since the strongest line of an allowed electronic transition is in general that vibronic transition in which the vibrational excitation does not change, the strongest line of the $S_2 \rightarrow S_0$ fluorescence should be the $S_{2,\nu_9} \rightarrow S_{0,\nu_9}$ transition at $28476 - 765$ cm^{-1} $= 27711$ cm^{-1} (cf. table 1). Unfortunately, at this wavenumber a clear distinction between the RF line or RR line of biphenylene and Raman lines of 3-methylpentane is not possible. Nevertheless one may estimate that the intensity of this line cannot be much stronger than the strongest identified RR line. With respect to the estimate of $\phi_{2\mathrm{f}}$ in section 3.1 that means, the contribution of the RF lines to the total emission spectrum cannot be larger than that estimated on the basis of the hypothetical $S_2 \rightarrow S_0$ fluorescence spectrum in fig. 5.

Table 2
Assignment of vibrational contour bands of the $S_0 \rightarrow S_2$ absorption band of biphenylene in 3-methylpentane at 100 K – see fig. 2. Notation ā, b̄, ...: see fig. 2; $\tilde{\nu}_{2,v}$: vibrational wavenumbers referring to the maximum of the origin band at 27850 cm^{-1}; n and ν_n: totally symmetric ground-state vibrations [27] – see table 1

	$\tilde{\nu}_{2,v}$ (cm^{-1})	ν_n (cm^{-1})	n
ā	395	395	10
b̄	755	765	9
c̄	1150	1166	6
		1160	9+10
d̄	1600	1530	9+9
		1561	6+10
		1666	3
ē	2335	2332	6+6
f̄	2760	2771	3+7

4. On the $S_1 \rightarrow S_0$ fluorescence

4.1. Vibrational analysis of the $S_1 \rightarrow S_0$ fluorescence spectrum

The purely electronic one-photon transition $S_{0,0}(A_g) \leftrightarrow S_{1,0}(B_{3g})$ of biphenylene is symmetry forbidden [15] and neither in absorption nor in emission observable. The position of $S_{1,0}$ can be determined by a vibrational analysis of the spectrum of the $S_1 \rightarrow S_0$ fluorescence. The spectrum consists of 23 distinct bands (see fig. 3 and table 3). The analysis of the spectrum is based on the following facts and assumptions:

(a) The striking feature of the spectrum is a recurring pattern of four bands (α_n, β_n, γ_n, δ_n) with $n = 1$, ..., 5. The obvious relation between ξ_n and ξ_{n+1} ($\xi = \alpha$, β, γ, δ) is

Table 3
Vibronic contour bands of the $S_1 \rightarrow S_0$ fluorescence from biphenylene in 3-methylpentane at 130 K – see fig. 3. Band positions were obtained with a maximum accuracy of ±5 $\mathrm{cm^{-1}}$ by taking the point of intersection of tangential lines drawn to the vibronic bands. The values of ξ'_n and ξ''_n were calculated with eqs. (20) and (21) and with $\tilde{\nu}_{0,0}$ defined by eq. (22)

Band	$\tilde{\nu}$ ($\mathrm{cm^{-1}}$)	$\tilde{\nu}-\xi'_n$ ($\mathrm{cm^{-1}}$)	$\tilde{\nu}-\xi''_n$ ($\mathrm{cm^{-1}}$)
($\tilde{\nu}_{0,0}$)	(23884)		
χ_1	23104		
χ_2	22632		
α_1	22215	+ 5	−31
β_1	21833	+18	−18
γ_1	21464	+19	−17
δ_1	21116	+11	−25
α_2	20748	0	−36
β_2	20375	+22	−34
γ_2	19998	+15	−21
δ_2	19651	+ 8	−28
α_3	19288	+ 2	−34
β_3	18916	+25	−11
γ_3	18546	+25	−11
δ_3	18202	+21	−15
α_4	17827	+ 3	−33
β_4	17458	+29	− 7
γ_4	17092	+33	− 3
δ_4	16751	+32	− 4
α_5	16382	+20	−16
β_5	16023	+26	−20
γ_5	15651	+46	+18
δ_5	15311	+54	+18
α_6	14926	+26	−10

$$\xi_n - \xi_{n+1} \approx \nu_4(\mathrm{a_g}) = 1462\ \mathrm{cm^{-1}}\ . \qquad (13)$$

(cf. tables 1 and 3).

(b) The β_n, γ_n, and δ_n roughly differ from the α_n by one quantum of an $\mathrm{a_g}$ vibration:

$$\alpha_n - \beta_n \approx \nu_{10}(\mathrm{a_g}) = 395\ \mathrm{cm^{-1}}\ , \qquad (14)$$

$$\alpha_n - \gamma_n \approx \nu_9(\mathrm{a_g}) = 765\ \mathrm{cm^{-1}}\ , \qquad (15)$$

$$\alpha_n - \delta_n \approx \nu_7(\mathrm{a_g}) = 1105\ \mathrm{cm^{-1}}\ . \qquad (16)$$

(c) The differences $\alpha_n - \beta_n$ and $\alpha_n - \gamma_n$ are significantly smaller than the fundamentals $\nu_{10}(\mathrm{a_g})$ and $\nu_9(\mathrm{a_g})$, respectively. Therefore, either the β and γ bands or the α and δ bands or all four kinds of bands do not represent single vibronic transitions.

(d) The structure of the observable part of the $S_0 \rightarrow S_1$ absorption band is similar to that of the $S_1 \rightarrow S_0$ fluorescence band. We tentatively assume that $S_{0,0} \rightarrow S_{1,\xi_n}$ absorption bands have similar relative strengths as $S_{1,0} \rightarrow S_{0,\xi_n}$ fluorescence bands. With this assumption we obtain the mirror-symmetric assignments $\bar{\xi}_n$ of the $S_0 \rightarrow S_1$ absorption band in fig. 2.

(e) By neglecting differences of vibrational fundamentals in S_0 and S_1 and other subtleties, we obtain with assumption (d) a first rough estimate $\tilde{\nu}_{0,0}^{(1)}$ of the position of $S_{1,0}$:

$$\tilde{\nu}_{0,0}^{(1)} = \tfrac{1}{2}(\bar{\alpha}_1 + \alpha_1) = 23830\ \mathrm{cm^{-1}}\ , \qquad (17)$$

where $\bar{\alpha} = 25445\ \mathrm{cm^{-1}}$ and $\alpha_1 = 22215\ \mathrm{cm^{-1}}$.

(f) With the assumption that $S_0 \rightarrow S_1$ absorption and $S_1 \rightarrow S_0$ fluorescence are induced by $\mathrm{b_{2u}}$ vibrations [15–19] follows that the difference $\tilde{\nu}_{0,0}^{(1)} - \alpha_1 = 1615\ \mathrm{cm^{-1}}$ should correspond either to one quantum of a $\mathrm{b_{2u}}$ vibration or to a combination of vibrations with the total symmetry $\mathrm{b_{2u}}$. We regard the following two assignments as the best:

$$\tilde{\nu}_{0,0} - \alpha_1 = \nu_{41}(\mathrm{b_{2u}}) + \nu_4(\mathrm{a_g}) = 1674\ \mathrm{cm^{-1}}\ , \qquad (18)$$

$$\tilde{\nu}_{0,0} - \alpha_1 = \nu_{35}(\mathrm{b_{2u}}) = 1638\ \mathrm{cm^{-1}}\ , \qquad (19)$$

where $\nu_{41}(\mathrm{B_{2u}}) = 212\ \mathrm{cm^{-1}}$ [27].

(g) From eqs. (18) and (19) follows that each of the four progressions ξ_n ($\xi = \alpha$, β, γ, δ) may result from the superposition of two progressions ξ'_n and ξ''_n,

$$\xi'_n = \tilde{\nu}_{0,0} - \nu_{41}(\mathrm{b_{2u}}) - \nu_4(\mathrm{a_g})n - \nu'_\xi(\mathrm{a_g})\ , \qquad (20)$$

$$\xi''_n = \tilde{\nu}_{0,0} - \nu_{35}(\mathrm{b_{2u}}) - \nu_4(\mathrm{a_g})(n-1) - \nu''_\xi(\mathrm{a_g})\ , \qquad (21)$$

where $\nu'_\alpha = \nu''_\alpha = 0$, $\nu'_\beta = \nu''_\beta = \nu_{10}(\mathrm{a_g})$, $\nu'_\gamma = \nu''_\gamma = \nu_9(\mathrm{a_g})$, and $\nu'_\delta = \nu''_\delta = \nu_7(\mathrm{a_g})$.

(h) From (c) and from eqs. (18) and (19) follows that the α bands – but not the β and γ bands – can be single vibronic transitions. We assume that the α bands are practically single vibronic transitions. By referring to α_2 as the most reliable α_n, we obtain as the best value of the 0, 0 transition:

$$\tilde{\nu}_{0,0} = \alpha_2 + \nu_{41}(\mathrm{b_{2u}}) + 2\nu_4(\mathrm{a_g}) = 23884\ \mathrm{cm^{-1}}\ . \qquad (22)$$

With this value of $\tilde{\nu}_{0,0}$, the values of ξ'_n and ξ''_n have been calculated. In table 3 the differences $\xi_n - \xi'_n$ and $\xi_n - \xi''_n$ are listed. In the range from α_1 to β_5, the experimental values ξ_n lie between ξ'_n and ξ''_n. Above α_5, the determination of the band positions is less reliable. In part the discrepancies may result from anharmonicity effects, which, however, should be small. As an example we consider anharmonicity in the α progression. We assume that only the vibrational ground state of S_1 is populated, and we neglect the possibility of Fermi resonances. The wavenumbers $\tilde{\nu}$ of observed vibronic bands are given by

$$\tilde{\nu}=\tilde{\nu}_{0,0}-\sum_i \omega_i^0 v_i-\sum_i \sum_{k\geqslant i} x_{ik}^0 v_i v_k-\ldots\,, \tag{23}$$

where the v_i are vibrational quantum numbers [57]. If higher than quadratic terms are neglected, the connection between the ω_i^0 and the observable fundamentals ν_i is given by

$$\omega_i^0=\nu_i-x_{ii}^0\,. \tag{24}$$

With $\nu_1\equiv\nu_{41}(b_{2u})$, $v_1=1$, $\nu_2\equiv\nu_4(a_g)$, and $v_2=n$, the α'_n terms are given by

$$\alpha_n=\tilde{\nu}_{0,0}-\nu_1-\nu_2 n-x_{22}^0 n(n-1)-x_{12}^0 n\,. \tag{25}$$

If we further assume $x_{12}^0\approx x_{22}^0$, then the anharmonicity correction for the α progression reduces to $\Delta\tilde{\nu}_{\mathrm{anh}}(\alpha'_n)\approx -x_{22}^0 n^2$. The comparison of the experimental α_n values with the calculated α'_n values yields

$$-1\ \mathrm{cm}^{-1}\lesssim x_{22}^0\leqslant 0\ \mathrm{cm}^{-1}\,. \tag{26}$$

Thus an anharmonicity correction of $\nu_{0,0}$ would be at most of the order of 5 cm^{-1}. In view of the accuracy of ± 10 cm^{-1} of experimental wavenumber differences, this correction can be neglected.

(i) With the fixing of $\tilde{\nu}_{0,0}$, the assignment of the bands χ_1 and χ_2 becomes possible, if the emitting state is $S_{1,0}$:

$$\tilde{\nu}_{0,0}-\chi_1=770\ \mathrm{cm}^{-1}\approx\nu_{40}(b_{2u})=751\ \mathrm{cm}^{-1}\,, \tag{27}$$

$$\tilde{\nu}_{0,0}-\chi_2=1252\ \mathrm{cm}^{-1}\approx\nu_{37}(b_{2u})=1267\ \mathrm{cm}^{-1}\,. \tag{28}$$

The comparison of the fluorescence spectra at 130 K (fig. 5) and at 293 K (fig. 6) reveals that the relative intensity of χ_1 and χ_2 increases with increasing temperature. Therefore, part of these bands is likely to be fluorescence from vibrationally excited S_1. One may assume that even at 130 K a substantial fraction of both bands is fluorescence from $S_{1,\nu_{41}}$. Thus, for example, $S_{1,\nu_{41}}\rightarrow S_{0,\nu_8}$ can contribute to χ_1, and $S_{1,\nu_{41}}\rightarrow S_{0,\nu_4}$ can contribute to ξ_2. Part of the background of the fluorescence spectrum and of observed band shifts must result from progressions built upon χ_1 and χ_2.

The vibrational analysis has shown that the observed distinct bands in the fluorescence spectrum can be interpreted in terms of four a_g vibrations and four b_{2u} vibrations (cf. table 4). This can be rationalized in terms of bond-order differences between S_0 and S_1 (cf. table 2 in ref. [1]). Because of the large changes of the bond orders of the C–C bonds a and b in the four-membered ring, only for those vibronic transitions large Franck–Condon factors are expected that are connected with appreciable changes of the lengths of the a bonds or b bonds or of both. In the force-field description of the in-plane vibrations of ref. [27], large changes of the lengths of the a bond and the b bond correspond to large contributions of the C–C potentials K_6 and K_5, respectively, to the potential energy distribution. An inspection of table 3 of ref. [27] shows that the observed a_g vibrations and the postulated b_{2u} vibrations are just those with the highest contribution of the K_6 potential. The importance of the progression-forming $\nu_4(a_g)$ vibration can be correlated with the fact that apart from K_6 also K_2, K_3 and K_4 yield large contributions to the potential energy distribution. The prominence of the $\nu_7(a_g)$ vibration can be correlated with the very large contribution of K_5 to the potential energy distribution.

Finally one may ask, to what extent other combinations of in-plane vibrations may contribute to the observable fluorescence. The combination of one b_{3g} vibration with one b_{1u} vibration has also the total symmetry b_{2u}. With respect to energy, the combination $\nu_{49}(b_{3g})=600\ \mathrm{cm}^{-1}$ with $\nu_{26}(b_{1u})=1019\ \mathrm{cm}^{-1}$ [27] could contribute to α_1. However, since for all b_{3g} and b_{1u} vibrations the contribution of K_6 to the potential energy distribution is small (< 15% – in table 3 of ref. [27] only contributions $\geqslant$ 15% are listed), this or other combinations of b_{3g} and b_{1u} vibrations are not likely to contribute substantially to the observed $S_1\rightarrow S_0$ fluorescence.

4.2. Polarization of the $S_1\rightarrow S_0$ fluorescence and orientational relaxation in S_1

In this part of our investigation, the first point of interest was the sign of the polarization degree P (see eq. (3)) of the $S_1\rightarrow S_0$ fluorescence from biphenylene in 3-methylpentane. We measured the polarized spectra $I_\parallel(\tilde{\nu})$ and $I_\perp(\tilde{\nu})$ of the $S_1\rightarrow S_0$ fluorescence at 130 K (at this temperature, fluorescence depolariza-

Table 4

Contribution of CC stretch coordinates to the potential energy distribution of the a_g and b_{2u} fundamentals that are likely to occur in the spectrum of the $S_1 \rightarrow S_0$ fluorescence from biphenylene (see fig. 3); the K_i are taken from table 3 of ref. [27]. The total bond-order changes ΔB_{total} in S_1 relative to S_0 and the bond notation a, b, ... are taken from table 2 of ref. [1] (see also fig. 2); the corresponding bond-order changes in the lowest triplet state T_1 [58] are needed in the following paper [2]

		CC bond				
		a	b	e	c	d
$\Delta B_{total}(S_1)$		0.299	−0.260	−0.190	−0.145	0.120
$\Delta B_{total}(T_1)$		0.198	−0.200	−0.204	−0.108	0.077
	Wavenumber (cm^{-1})	K_6 (%)	K_5 (%)	K_4 (%)	K_2 (%)	K_3 (%)
$\nu_4(a_g)$	1462	19		35	26	24
$\nu_7(a_g)$	1105	20	58			31
$\nu_9(a_g)$	765	16		31		
$\nu_{10}(a_g)$	395	29			16	
$\nu_{35}(b_{2u})$	1638	22			52	17
$\nu_{37}(b_{2u})$	1267	18				
$\nu_{40}(b_{2u})$	751	17				
$\nu_{41}(b_{2u})$	212	24				

tion due to orientational relaxation is still small), and we calculated with eq. (3) the fluorescence polarization spectrum $P(\tilde{\nu})$ depicted in fig. 7. P is positive – as expected for an S_1 fluorescence resulting from dominant S_1–S_2 vibronic coupling – and in agreement with the results obtained by Shizuka et al. [59] with biphenylene powder. The deviations of $P(\tilde{\nu})$ from a constant value indicate that, apart from S_1–S_2 vibronic coupling, other types of vibronic coupling may contribute to the observable $S_1 \rightarrow S_0$ fluorescence.

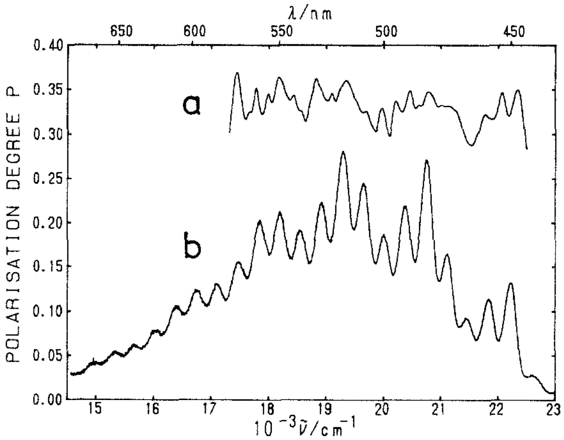

Fig. 7. (a) Polarization spectrum $P(\tilde{\nu})$ and (b) spectrum of the $S_1 \rightarrow S_0$ fluorescence from biphenylene in 3-methylpentane at 130 K. Some of the minor details of the structure of $P(\tilde{\nu})$ are due to noise, but the deviation of P from a constant value is beyond doubt.

The main aim of our fluorescence-polarization experiments has been to determine the orientational relaxation time τ_{or} of biphenylene in S_1 from the dependence of P on the ratio η/T of the viscosity η and the temperature T. The simplest relation between τ_{or} and η/T is given by Perrin's formula for spherical particles [20] which is written here in a slightly modified form,

$$P=P_0[1+(1-\tfrac{1}{3}P_0)\tau_1/\tau_{or}]^{-1}, \qquad (29)$$

where P_0 is the value of P corresponding to infinite viscosity and τ_1 is the lifetime of S_1 as before. For a spherical particle with volume v_s, τ_{or} is given by

$$\tau_{or}=\frac{1}{6D_{rot}}=\frac{\eta}{k_B T}v_s, \qquad (30)$$

where D_{rot} is the rotational diffusion coefficient and k_B is the Boltzmann constant.

We measured the temperature dependence of P at 20800 cm^{-1} (maximum of uncorrected fluorescence spectrum); the values of P are listed in table 5. The

Table 5
Polarization degree P of the $S_1 \rightarrow S_0$ fluorescence at 20800 cm^{-1} from biphenylene in 3-methylpentane as function of the temperature T and the solvent viscosity η. The temperature was measured with a calibrated thermocouple with an absolute accuracy of ±0.5 K. The accuracy of the values of P is ±0.010. The values of η were calculated with eq. (4)

T(K)	P	η (cP)
128.6	0.340	38.47
129.9	0.330	32.90
133.9	0.300	21.41
137.0	0.278	16.06
140.4	0.253	12.15
144.5	0.218	9.04
148.6	0.188	6.98
154.1	0.155	5.16
162.5	0.114	3.515
168.7	0.091	2.764
175.8	0.073	2.172
183.0	0.061	1.752
193.2	0.047	1.343
209.9	0.033	0.935
222.5	0.026	0.742
270.9	0.017	0.381

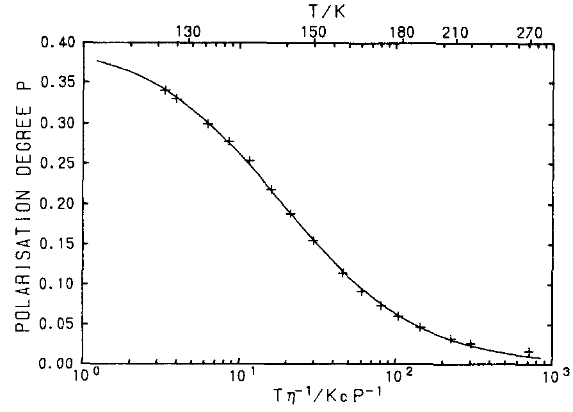

Fig. 8. Polarization degree P at 20800 cm^{-1} of the $S_1 \rightarrow S_0$ fluorescence from biphenylene in 3-methylpentane as function of T/η; the curve has been calculated with eqs. (29) and (30) and with the parameter values given in section 4.2.

observed dependence of P on η/T is rather accurately described by Perrin's formula (29). By fitting eq. (29) to the experimental values of $P(T)$ with $\eta(T)$ from eq. (4) we obtained $P_0 = 0.401 \pm 0.010$, and with $\tau_1 = 240 \pm 20$ ps [60],

$$v_s = (5.4 \pm 0.4) \times 10^{-23}\,\mathrm{cm}^3 . \qquad (31)$$

The value of P_0 is close to the theoretical maximum 0.5. In fig. 8 the fitted curve $P = P(T/\eta)$ is compared with the experimental value of P.

The accurate description of the experimental data by eq. (29) may seem surprising for two reasons. Firstly, in general the orientational relaxation of non-spherical particles can no longer be described by a *single* orientational relaxation time [55,61,62]. Secondly, even if eq. (29) is applicable in the present case, the temperature independence of τ_1 between 129 and 271 K is not self-evident. In the following we first show that τ_1 can at most weakly depend on the temperature and then discuss the implications of the validity of eq. (29).

Let τ_1' and τ_1'' be the lifetimes of S_1 at 130 and 293 K, respectively. We base an estimate of τ_1''/τ_1' on a quantitative comparison of the emission spectra in figs. 5 and 6 and on the fact that the radiative lifetime τ_{1r} of S_1 is much longer than τ_1. For τ_1''/τ_1' the following relation can be derived:

$$\frac{\tau_1''}{\tau_1'} \approx \frac{I_{1f}'' f_c}{I_{1f}'} \frac{\epsilon' \rho' n_f'^3}{\epsilon'' \rho'' n_f''^3} \frac{(n_{RS}''+2)^2/n_{RS}''}{(n_{RS}'+2)^2/n_{RS}'} . \qquad (32)$$

The three factors on the right side of eq. (32) have the following meaning: $(I_{1f}''/I_{1f}')f_c$ is the ratio of the integrated $S_1 \rightarrow S_0$ fluorescence bands times a correction factor f_c taking account of the different values of P at the two temperatures (I_{1f}'' and I_{1f}' refer to spectra which are normalized to equal integrated intensity of the C–H Raman bands). The second factor takes account of the temperature dependence of the following quantities: the molar extinction coefficient ϵ of biphenylene at the excitation wavenumber, the concentration of biphenylene, which is proportional to the density ϱ of the solvent, and the radiative lifetime τ_{1r}, which depends on the refractive index n_f of the solvent in the range of the $S_1 \rightarrow S_0$ fluorescence (a solvent-independent value of the $S_0 \rightarrow S_1$ oscillator strength is assumed – cf. sections 3.7 and 4.3 in ref. [29]). The third factor $F(n_{RS})$ takes account of the temperature dependence of the Raman scattering (RS) [63]. With $I_{1f}''/I_{1f}' = 0.72$, $f_c \approx 1.1$, $\epsilon'/\epsilon'' \approx 0.9$, $\rho'/\rho'' = 1.21$, $(n_f'/n_f'')^3 \approx 1.22$, and $F(n_{RS}) \approx 0.93$, we obtain

$$\tau_1''/\tau_1' = 1.0 \pm 0.2 . \qquad (33)$$

In accord with this estimate, no significant improvement of the fitting of eq. (29) to the experimental values of P was achieved by treating τ_1 as a temperature-dependent fitting parameter. Moreover, if τ_1 would increase by $\approx 20\%$ upon decreasing the temperature from 293 to 130 K, most of this increase should take place at temperatures > 210 K, where P is already very small. Thus, on the basis of the available data, the assumption of a temperature-independent τ_1 is justified.

With respect to the application of eq. (29) to *nonspherical* particles, Memming [64] has shown that eq. (29) is still valid for a rotational ellipsoid, if at least one of the optical transitions implied (absorption or emission) is polarized in the direction of the rotational axis of the ellipsoid. For the present purpose, a prolate rotational ellipsoid should be a good model for the orientational relaxation of biphenylene. Let z be the rotational axis of the ellipsoid and x and y be the two equivalent axes perpendicular to z. Then for the rotational diffusion coefficients the relation $D_x = D_y < D_z$ holds. For a z-polarized fluorescence only rotations about the x axis and the y axis contribute to fluorescence depolarization; the corresponding orientational relaxation time [64] is

$$\tau_{\mathrm{or}} = \frac{\eta}{k_{\mathrm{B}} T} \frac{v_e}{\Phi'_x} , \qquad (34)$$

where $v_{\mathrm{e}} = \frac{4}{3}\pi a b^2$ is the volume of a rotational ellipsoid with half axis a and radius b, and Φ'_x is a function of the ratio $\gamma = b/a$ (Φ'_x is related to Φ_x in ref. [64] by $\Phi'_x = \frac{3}{4}\Phi_x$). Φ'_x is equal to unity for a spherical particle ($\gamma = 1$); for $\gamma < 1$ (cf. eq. (44) in ref. [64]):

$$\Phi'_x = \tfrac{3}{4}\{(2-\gamma^2)\ln[(1+\delta)/(1-\delta)] - 2\delta\} \times (1+\gamma^2)^{-1}\gamma^2\delta^{-3} , \qquad (35)$$

where

$$\delta = (1-\gamma^2)^{1/2} . \qquad (36)$$

For biphenylene we assume $\gamma = 0.5$ or $\Phi'_x = 0.664$ and obtain

$$v_{\mathrm{e}} = \Phi'_x v_{\mathrm{s}} = 3.6 \times 10^{-23}\ \mathrm{cm}^3 . \qquad (37)$$

The value of v_{e} can be compared with the molecular volume $v'_{\mathrm{e}} = 14.9 \times 10^{-23}$ cm^3 obtained from the molar mass and the density of solid biphenylene at room temperature by assuming a space-filling factor of 0.74. The difference between v_{e} and v'_{e} corresponds to a factor

$$a/a' = (v_{\mathrm{e}}/v'_{\mathrm{e}})^{1/3} = 0.62 , \qquad (38)$$

by which the linear dimensions of the biphenylene molecule obtained from fluorescence depolarization are too small. This discrepancy is in accord with a similar discrepancy known for translational diffusion coefficients. As an example we take the diffusion coefficient $\bar{D}$ of ^{3}anthracene* in hexane [65]. We assume again that a rotational ellipsoid with $\gamma = 0.5$ is a good model for the present purpose. According to Perrin [62] the translational diffusion coefficient $\bar{D}_{\mathrm{e}}$ of a rotational ellipsoid with $\gamma < 1$ is given by

$$\bar{D}_{\mathrm{e}} = \bar{D}_{\mathrm{s}}\{\gamma^{2/3}(2\delta)^{-1}\ln[(1+\delta)/(1-\delta)]\} , \qquad (39)$$

where $\bar{D}_{\mathrm{s}} = k_{\mathrm{B}}T/6\pi\eta a \gamma^{2/3}$ is the diffusion coefficient of spherical particles of the same volume (for the factor {...} in eq. (39) cf. ref. [64], p. 180). For ^{3}anthracene* in hexane at 298 K ($\eta = 0.298$ cP), the experimental value is $\bar{D}_{\mathrm{e}} = 3.2 \times 10^{-5}$ cm^2 s^{-1} [65], corresponding to $a = 3.5 \times 10^{-8}$ cm for $\gamma = 0.5$. From the molecular volume v'_{e} (estimated as above for biphenylene) $a' = 5.9 \times 10^{-8}$ cm is obtained. The resulting ratio $a/a' = 0.59$ is close to that obtained for biphenylene in 3-methylpentane. The result of this comparison of rotational and translational diffusion coefficients can be regarded as an additional confirmation of an at most weak dependence of τ_1 on temperature.

Orientational relaxation times can be directly measured with time-resolved spectroscopy [55]. In connection with the preceding considerations, the work by von Jena and Lessing [66] is of particular interest. According to these authors, even with less symmetrical molecules than biphenylene, orientational relaxation can be described with a *single* relaxation time, if the orientational relaxation is probed by an optical transition polarized in the direction of the long axis of a molecule. Thus their results justify the present simplified treatment of orientational relaxation of biphenylene.

Our results are a further confirmation of the well-known fact that, for a given solvent, rotational or translational diffusion coefficients of solute molecules are rather accurately proportional to T/η, although the molecular volume obtained with eqs. (29)

and (30) or the average radius obtained with the Stokes–Einstein equation may substantially deviate from their true values [55,65,67]. On the other hand, upon variation of η by changing the solvent or the composition of a solvent mixture, substantial deviations from this proportionality are often observed [55,65,67,68].

In conclusion, eqs. (30) and (31) should yield the orientational relaxation time of biphenylene in 3-methylpentane and similar solvents with an accuracy of ±20%, if only rotation about the short molecular axis is important for the observed quantity. The slight uncertainty in the temperature dependence of τ_1 means that the value of the effective molecular volume v_s in eq. (31) may be too small by $\lesssim 20\%$. Values of τ_{or} calculated with eqs. (30) and (31) may be too small by the same amount.

Finally we give three values of τ_{or}. Biphenylene in 3-methylpentane: $\tau_{or}(130\ \mathrm{K}) \approx 1.0 \pm 0.2$ ns and $\tau_{or}(293\ \mathrm{K}) \approx 4 \pm 1$ ps. In connection with ref. [1], the value of τ_{or} of biphenylene in cyclohexane at 293 K is of interest. With $\eta(293\ \mathrm{K}) = 0.98 \times 10^{-2}$ P follows $\tau_{or} \approx 13 \pm 3$ ps; a directly determined value of τ_{or} is not yet known (in the experiments of ref. [1], effects of orientational relaxation have been deliberately eliminated by using a magic-angle setup).

5. Summary and conclusions

(1) Upon $S_0 \rightarrow S_2$ photoexcitation of biphenylene in liquid 3-methylpentane, no prompt $S_2 \rightarrow S_0$ fluorescence was observed because of the much stronger Raman-scattered light.

(2) Eight resonance Raman lines of biphenylene have been identified and assigned to totally symmetric vibrations.

(3) An upper limit $\phi_{2f} \approx 1 \times 10^{-6}$ is estimated for the quantum yield of the prompt $S_2 \rightarrow S_0$ fluorescence.

(4) Biphenylene is an example of intermediate *strong* S_2–S_1 coupling. In this case, for the radiative lifetime τ_{2r}^* of S_2 calculated from the $S_0 \rightarrow S_2$ absorption band and the true radiative lifetime τ_{2r} the relation $\tau_{2r}^* \ll \tau_{2r}$ may hold. Therefore, from $\tau_{2r}^* \approx 16$ ns and $\phi_{2f} \lesssim 1 \times 10^{-6}$ does not follow an ultrashort lifetime ($\lesssim 20$ fs) of S_2.

(5) At high spectral resolution, a distinction between $S_2 \rightarrow S_0$ resonance fluorescence lines and resonance Raman lines of biphenylene in 3-methylpentane at 130 K should be possible.

(6) The vibrational analysis of the $S_1 \rightarrow S_0$ fluorescence from biphenylene yields $\approx 23900\ \mathrm{cm}^{-1}$ for the position of $S_{1,0}$.

(7) The $S_1 \rightarrow S_0$ fluorescence from biphenylene has the same long-axis polarization as the $S_0 \rightarrow S_2$ absorption band.

(8) The dependence of the polarization degree of the $S_1 \rightarrow S_0$ fluorescence on temperature and viscosity can be described with Perrin's formula which allows one to calculate orientational relaxation times of biphenylene in S_1.

(9) The lifetime of S_1 of biphenylene in 3-methylpentane is within ±20% constant between 130 and 293 K.

Acknowledgement

BN thanks Professor W. Lüttke for drawing our attention to the problem of the lifetime of S_2 of biphenylene, for stimulating discussions, and for very valuable comments on the manuscript. We thank Professor A. Weller for support, Mr. M. Niemeyer for the preparation and purification of biphenylene and for discussions, Mr. H. Lesche for the measurement of the viscosity and the density of 3-methylpentane and for the preparation of samples, Mr. M. Lindrum for making his absorption spectrometer available to us and for valuable help in other respects, and Dr. B. Dick for comments on the manuscript. Support by the Deutsche Forschungsgemeinschaft (Sonderforschungsbereich 93, Photochemie mit Lasern) is gratefully acknowledged. Finally we thank the referees for valuable comments and suggestions.

References

[1] T. Elsaesser, F. Lärmer, W. Kaiser, B. Dick, M. Niemeyer and W. Lüttke, Chem. Phys. 126 (1988) 405.
[2] J. Hertzberg and B. Nickel, Chem. Phys. 132 (1989) 235.
[3] S.J. Strickler and R.A. Berg, J. Chem. Phys. 37 (1962) 814.
[4] M. Kasha, Discussions Faraday Soc. 9 (1950) 14.
[5] R.J. Watts and S.J. Strickler, J. Chem. Phys. 44 (1966) 2423.
[6] P.A. Geldof, R.P.H. Rettschnick and G.J. Hoytink, Chem. Phys. Letters 4 (1969) 59.

[7] J.L. Richards and S.A. Rice, Chem. Phys. Letters 9 (1971) 444.

[8] F. Hirayama, T.A. Gregory and S. Lipsky, J. Chem. Phys. 58 (1973) 4696.

[9] B. Nickel, Helv. Chim. Acta 61 (1978) 198.

[10] I. Kaplan and J. Jortner, Chem. Phys. 32 (1978) 381.

[11] M.R. Topp, H.-B. Lin and K.-J. Choi, Chem. Phys. 60 (1981) 47.

[12] V.A. Lyubimtsev and V.L. Ermolaev, Opt. i Spectroskopiya 61 (1986) 511.

[13] B. Dick and B. Nickel, Chem. Phys. 110 (1986) 131.

[14] R.S. Mulliken, J. Chem. Phys. 23 (1955) 1997.

[15] R.M. Hochstrasser, J. Chem. Phys. 33 (1960) 950.

[16] R.M. Hochstrasser, Can. J. Chem. 39 (1961) 765,

[17] I. Zanon, J. Chem. Soc. Faraday Trans. II 69 (1973) 1164.

[18] T. Hoshi, H. Yamamoto, T. Miyauchi, S. Mori, M. Kobayashi and Y. Tanizaki, Ber. Bunsenges. Physik. Chem. 86 (1982) 330.

[19] G. Fischer, Vibronic Coupling (Academic Press, New York, 1984).

[20] F. Perrin, J. Phys. (Paris) 7 (1926) 390.

[21] M. Lindrum, Diplomarbeit, Universität Göttingen, FRG (1987).

[22] B. Nickel and G. Roden, Ber. Bunsenges. Physik. Chem. 81 (1977) 281.

[23] B. Nickel and M.F. Rodríguez Prieto, Z. Physik. Chem. NF 150 (1986) 31.

[24] D. Klemp and B. Nickel, Chem. Phys. Letters 130 (1986) 493.

[25] H. Lesche, D. Klemp and B. Nickel, Z. Physik. Chem. NF 141 (1984) 239.

[26] The International Practical Temperature Scale of 1968, Metrologia 5 (1969) 35.

[27] A. Girlando and C. Pecile, J. Chem. Soc. Faraday Trans. II 69 (1973) 818.

[28] Th. Förster, Fluoreszenz Organischer Verbindungen (Vandenhoeck & Ruprecht, Göttingen, 1951).

[29] J.B. Birks, Photophysics of Aromatic Molecules (Wiley-Interscience, New York, 1970).

[30] A. Amirav, M. Sonnenschein and J. Jortner, J. Phys. Chem. 88 (1984) 5593.

[31] J. Jortner, S.A. Rice and R. Hochstrasser, Advan. Photochem. 7 (1969) 149.

[32] J. Jortner and S. Mukamel, Preparation and Decay of Excited Molecular States, in: The World of Quantum Chemistry, eds. R. Daudel and B. Pullman (Reidel, Dordrecht, 1974) p. 145; sect. 15.

[33] A. Tramer and R. Voltz, Excited States, Vol. 4. Time-Resolved Studies of Excited Molecules, ed. E.C. Lim (Academic Press, New York, 1979) p. 281; sect. b, p. 367.

[34] A. Nitzan, J. Jortner and P.M. Rentzepis, Proc. Roy. Soc. A 327 (1972) 367, 386.

[35] A. Amirav, U. Even and J. Jortner, J. Chem. Phys. 74 (1981) 3745.

[36] D.S. McClure, J. Chem. Phys. 22 (1954) 1668.

[37] J. Wessel and D.S. McClure, Mol. Cryst. Liquid Cryst. 58 (1980) 121.

[38] G.W. Robinson and C.A. Langhoff, Chem. Phys. 5 (1974) 1.

[39] C.A. Langhoff and G.W. Robinson, Chem. Phys. 6 (1974) 34.

[40] G. Fischer, Topics Current Chem. 66 (1976) 115.

[41] P. Wannier, P.M. Rentzepis and J. Jortner, Chem. Phys. Letters 10 (1971) 102.

[42] P. Wannier, P.M. Rentzepis and J. Jortner, Chem. Phys. Letters 10 (1971) 193.

[43] A.E. Douglas, J. Chem. Phys. 45 (1966) 1007.

[44] J.M. Blondeau and M. Stockburger, Chem. Phys. Letters 8 (1971) 436.

[45] T. Deinum, C.J. Werkhoven, J. Langelaar, R.P.H. Rettschnick and J.D.W. van Voorst,, Chem. Phys. Letters 19 (1973) 29.

[46] S.M. Beck, J.B. Hopkins, D.E. Powers and R.E. Smalley, J. Chem. Phys. 74 (1981) 43.

[47] S.M. Beck, D.E. Powers, J.B. Hopkins and R.E. Smalley, J. Chem. Phys. 73 (1980) 2019.

[48] G. Fischer, Chem. Phys. 4 (1974) 62.

[49] R.M. Hochstrasser and R.D. McAlpine, J. Chem. Phys. 44 (1966) 3325.

[50] T.C. Felder, K.-J. Choi and M.R. Topp, Chem. Phys. 64 (1982) 175.

[51] P.C. Alford and T.F. Palmer, J. Chem. Soc. Faraday Trans. II 79 (1983) 433.

[52] T. Itoh and B.E. Kohler, J. Phys. Chem. 91 (1987) 1760.

[53] B.E. Kohler and T.A. Spiglanin, J. Chem. Phys. 80 (1984) 5465.

[54] C. Rulliere, A. Declemy and Ph. Kottis, Chem. Phys. Letters 110 (1984) 308.

[55] G.R. Fleming, Chemical Applications of Ultrafast Spectroscopy (Oxford Univ. Press, Oxford, 1986).

[56] J. Friedrich and D. Haarer, Angew. Chem. 96 (1984) 96; Angew. Chem. Intern. Ed. 23 (1984) 113.

[57] G. Herzberg, Molecular Spectra and Molecular Structure, Vol. 3. Electronic Spectra and Electronic Structure of Polyatomic Molecules (Van Nostrand, Princeton, 1967), eq. (II, 25) p. 142.

[58] B. Dick, private communication.

[59] H. Shizuka, T. Ogiwara, S. Cho and T. Morita, Chem. Phys. Letters 42 (1976) 311.

[60] H.-B. Lin and M. Topp, Chem. Phys. Letters 64 (1979) 452.

[61] F. Perrin, J. Phys. (Paris) 5 (1934) 497.

[62] F. Perrin, J. Phys. (Paris) 7 (1936) 1.

[63] J. Brandmüller and H. Moser, Einführung in die Ramanspektroskopie (Steinkopff, Darmstadt, 1962) p. 240.

[64] R. Memming, Z. Physik. Chem. NF 28 (1961) 168.

[65] E.G. Meyer and B. Nickel, Z. Naturforsch. 35a (1980) 503.

[66] A. von Jena and H.E. Lessing, Ber. Bunsenges. Physik. Chem. 83 (1979) 181.

[67] D.H. Waldeck and G.R. Fleming, J. Phys. Chem. 85 (1981) 2614.

[68] S. Canonica, A.A. Schmid and U.P. Wild, Chem. Phys. Letters 122 (1985) 529.